This article has been accepted for publication in IEEE Transactions on Biomedical Engineering. This is the author's version which has not been fully edited and content may change prior to final publication. Citation information: DOI 10.1109/TBME.2023.3277546

Prediction of Stroke Onset Time with Combined Fast High-Resolution Magnetic Resonance Spectroscopic and Quantitative T_2 Mapping

Ziyu Meng, *Student Member*, *IEEE*, Rong Guo, *Member*, *IEEE*, Tianyao Wang, Bin Bo, Zengping Lin, Yudu Li, *Student Member*, *IEEE*, Yibo Zhao, *Student Member*, *IEEE*, Xin Yu, David J. Lin, Parashkev Nachev, Zhi-Pei Liang, *Fellow*, *IEEE*, and Yao Li*, *Senior Member*, *IEEE*

***Abstract*— *Objective:* The purpose of this work is to develop a multispectral imaging approach that combines fast high-resolution 3D magnetic resonance spectroscopic imaging (MRSI) and fast quantitative T_2 mapping to capture the multifactorial biochemical changes within stroke lesions and evaluate its potentials for stroke onset time prediction. *Methods:* Special imaging sequences combining fast trajectories and sparse sampling were used to obtain whole-brain maps of both neurometabolites ($2.0\times3.0\times3.0$ mm^3) and quantitative T_2 values ($1.9\times1.9\times3.0$ mm^3) within a 9-minute scan. Participants with ischemic stroke at hyperacute (0–24h, n=23) or acute (24h–7d, n=33) phase were recruited in this study. Lesion N-acetylaspartate (NAA), lactate, choline, creatine, and T_2 signals were compared between groups and correlated with patient symptomatic duration. Bayesian regression analyses were employed to compare the predictive models of symptomatic duration using multispectral signals. *Results:* In both groups, increased T_2 and lactate levels, as well as decreased NAA and choline levels were detected within the lesion (all p<0.001). Changes in T_2, NAA, choline, and creatine signals were correlated with symptomatic duration for all patients (all p<0.005). Predictive models of stroke onset time combining signals from MRSI and T_2 mapping achieved the best performance (hyperacute: R^2=0.438; all: R^2=0.548). *Conclusion:* The proposed multispectral imaging approach provides a combination of biomarkers that index early pathological changes after stroke in a clinical-feasible time and improves the assessment of the duration of cerebral infarction. *Significance:* Developing accurate and efficient neuroimaging techniques to provide sensitive biomarkers for prediction of stroke onset time is of great importance for maximizing the proportion of patients eligible for therapeutic intervention. The proposed method provides a clinically feasible tool for the assessment of symptom onset time post ischemic stroke, which will help guide time-sensitive clinical management.**

***Index Terms*— ischemic stroke; magnetic resonance spectroscopic imaging; T_2 mapping; stroke onset time**

I. Introduction

DETERMING the temporal onset of ischemic stroke is critical to establishing the therapeutic window – currently 4.5 hours for thrombolysis, and 6 hours for intra-arterial recanalization – on which treatment selection depends [1]. Approximately 30% of stroke patients present with an unknown time of onset, rendering them ineligible for thrombolytic therapy [2]. Therefore, developing neuroimaging techniques to provide sensitive biomarkers for prediction of symptom onset time to maximize the proportion of patients eligible for therapeutic intervention is of great importance.

Magnetic resonance spectroscopic imaging (MRSI) provides a powerful tool for non-invasive measurement of the neurometabolic changes induced by stroke, which provide a direct index of the progression of brain tissue injury over time [3], [4]. With ^{1}H-MRSI, we can simultaneously measure the multiple metabolites involved in the cascading metabolic effects that ischemia induces, including decreased N-acetylaspartate (NAA) as a marker of neuronal loss and increased lactate as a marker of anaerobic glycolysis and tissue acidosis [4]. Quantitative T_2 mapping provides sensitive biomarkers to the subtle pathological changes in acute stroke,

Z. Meng is with School of Biomedical Engineering, Shanghai Jiao Tong University, Shanghai, China. R. Guo is with Beckman Institute for Advanced Science and Technology, University of Illinois at Urbana-Champaign, Urbana, IL, USA, and is also with Siemens Medical Solutions USA, Inc., Urbana, IL, USA. T. Wang is with Radiology Department, Shanghai Fifth People's Hospital, Shanghai, China. B. Bo and Z. Lin, are with School of Biomedical Engineering, Shanghai Jiao Tong University, Shanghai, China. Y. Li is with Beckman Institute for Advanced Science and Technology, University of Illinois at Urbana-Champaign, Urbana, IL, USA, and is also with National Center for Supercomputing Applications, University of Illinois at Urbana-Champaign, Urbana, IL, USA. Y. Zhao is with Beckman Institute for Advanced Science and Technology, University of Illinois at Urbana-Champaign, Urbana, IL, USA, and is also with Department of Electrical and Computer Engineering, University of Illinois at Urbana-Champaign, Urbana, IL, USA. X. Yu is with Department of Biomedical Engineering, Case Western Reserve University, Cleveland, OH, USA. D. J. Lin is with Department of Neurology, Massachusetts General Hospital, Harvard Medical School, Boston, MA, USA. P. Nachev is with High-Dimensional Neurology Group, Institute of Neurology, University College London, London, United Kingdom. Z.-P. Liang is with Beckman Institute for Advanced Science and Technology, University of Illinois at Urbana-Champaign, Urbana, IL, USA, and is also with Department of Electrical and Computer Engineering, University of Illinois at Urbana-Champaign, Urbana, IL, USA. *Y. Li is with School of Biomedical Engineering, Shanghai Jiao Tong University, Shanghai, China (correspondence e-mail: yaoli@sjtu.edu.cn).

This work was supported by Shanghai Pilot Program for Basic Research-Shanghai Jiao Tong University (No. 21TQ1400203); National Natural Science Foundation of China (No. 81871083) and Shanghai Jiao Tong University Scientific and Technological Innovation Funds (2019QYA12); Key Program of Multidisciplinary Cross Research Foundation of Shanghai Jiao Tong University (YG2021ZD28, YG2023ZD22). PN is funded by the Wellcome Trust (213038/Z/18/Z) and the UCLH NIHR Biomedical Research Centre.

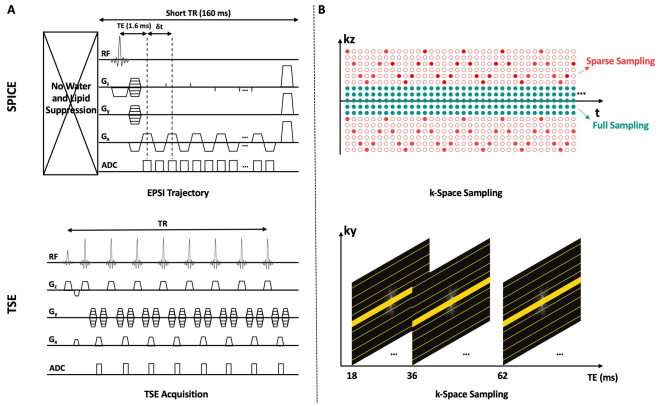

Fig. 1. Data acquisition scheme for fast 3D MRSI and quantitative T_2 mapping. (A) Sequence design. The SPectroscopic Imaging by exploiting spatiospectral CorrElation (SPICE) sequence uses an echo planar spectroscopic imaging (EPSI) trajectory for rapid encoding. The turbo spin echo (TSE) sequence uses multiple spin echoes to provide an increased number of k-space encodings in each excitation. (B) k-space sampling pattern. SPICE uses a variable-density sampling strategy, with central (k, t)-space fully sampled and peripheral (k, t)-space sparsely sampled. The TSE sequence uses a factor of 3 under-sampling in ky direction, and only three TEs (echo times) were acquired.

which showed improved accuracy in predicting time post symptom onset (< 3h) than fluid-attenuated inversion recovery (FLAIR) imaging [5].

However, both 3D MRSI and quantitative T_2 mapping suffer from long acquisition times, low spatial resolutions, and narrow tissue coverage, which significantly limited their clinical applications in acute stroke [3], [6]–[8]. In clinical practice, the most commonly used MRSI technique is the chemical shift imaging (CSI) sequence, which typically acquires a single slice with a resolution at around 10 mm in 15 minutes [4], [6], [9]. The state-of-the-art fast MRSI techniques have shown imaging capabilities of achieving resolutions around 5 mm in around 25-minute scan times [10], which does not fully address the clinical needs for stroke metabolic imaging. For quantitative T_2 mapping, spin echo (SE)-based methods require the acquisition of a sequence of T_2-weighted images with different echo times (TEs), leading to over 10-minute acquisition times. Turbo spin echo (TSE)-based methods are often used in the clinical settings due to their high imaging speeds. However, imperfections in the refocusing pulses used and the resulting stimulated echoes would bias the T_2 estimation using a simple exponential curve fitting of TSE data [11]–[13]. Therefore, till now combined fast high-resolution 3D MRSI and quantitative T_2 mapping have not been successfully demonstrated in the clinical settings and its potential clinical value for stroke imaging has not been explored.

Here we presented a multispectral imaging approach that combines fast high-resolution 3D MRSI ($2.0 \times 3.0 \times 3.0$ mm^3; 8 min) and fast quantitative T_2 mapping ($1.9 \times 1.9 \times 3.0$ mm^3; 69 sec) to capture the multifactorial biochemical changes within the ischemic lesions. In data acquisition, the SPectroscopic Imaging by exploiting spatiospectral CorrElation (SPICE) [14]–[21] sequence with rapid echo planar spectroscopic imaging (EPSI) trajectory and sparse sampling was used for fast MRSI; and a TSE sequence with parallel imaging and only three TEs was used for fast quantitative T_2 mapping. In data processing, a subspace-based method was used for reconstruction of metabolite signals and a model-based method was used for correcting T_2 estimation bias. We demonstrated the feasibility of concurrent whole-brain mapping of NAA, lactate, choline, creatine, and quantitative T_2 within about 9-minute scanning time in the clinical settings. Moreover, the potentials of such a multispectral imaging technique for the prediction of symptomatic duration of ischemia has been shown, in a cohort of 56 acute stroke patients. The combination of signals from high-resolution MRSI and quantitative T_2 mapping achieved good performance in predicting stroke onset time, which has good potential to help guide clinical management of stroke.

II. METHODS

A. Data Acquisition

To enable MRSI and T_2 mapping in a clinically feasible time, the SPICE sequence and TSE sequence were used, which, as illustrated in Fig. 1, use fast-scanning trajectories and sparse sampling to achieve high imaging speeds.

The SPICE sequence used the EPSI trajectory to provide rapid spatial and temporal encodings simultaneously, while the TSE sequence used the multiple refocused echoes for increased number of spatial encodings in each excitation. More specifically, the EPSI trajectory in the SPICE sequence used 110 spatial encodings with a large echospacing (1.76 ms), which provided an acceleration factor of 110 compared with typical CSI readouts. The TSE sequence was implemented with a turbo factor of 8, that is, 8 lines of k-space were encoded after each excitation, providing 8 times higher imaging efficiency than the conventional single-TE SE sequences. Sparse sampling was employed in both sequences. For the SPICE sequence, only central k-space was fully sampled to preserve signal-to-noise (SNR) for the metabolites while peripheral k-space was sparsely sampled using spatiotemporal CAIPIRINHA sampling with under-sampling factors of 3 in ky and 12 in (kz, t)-space [22]. For the TSE sequence, a factor of 3 under-sampling was used in ky, and only 3 TEs (18, 36, 62 ms) were acquired to encode the T_2 relaxation, which was much fewer than the typical T_2 mapping sequences with more than 10 TEs. We selected TE values shorter than 80 ms in order to capture the T_2 decay of brain tissues with the shortest T_2 value of around 80 ms for the white matter.

In addition to rapid and sparse sampling, the SPICE sequence also has several other special data acquisition features that help improve imaging efficiency and robustness, which include: a) removal of water and lipid suppression pulses, b) use of free induction decay (FID)-based acquisition with short repetition time (TR) (160 ms) and ultrashort TE (1.6 ms), which significantly enhance imaging speed and SNR efficiency, and c) embedding navigators for tracking subject motion and field drifts during the scan. As a result, the SPICE sequence was able to achieve: $2.0 \times 3.0 \times 3.0$ mm^3 nominal resolution, covering a field of view (FOV) of $240 \times 240 \times 72$ mm^3 in 8-minute scan time for metabolic imaging. For T_2 mapping, our TSE sequence was able to achieve $1.9 \times 1.9 \times 3.0$ mm^3 resolution in only 69 seconds (TR = 5030 ms, FOV = $240 \times 240 \times 72$ mm^3), in

contrast to conventional clinical T_2 mapping scans that often require more than 10 minutes [23].

B. Data Processing

1) Neurometabolites Mapping

The data acquisition scheme for fast high-resolution metabolic imaging may lead to low SNR and spectral aliasing artifacts if not properly handled. To avoid these problems, we used a union-of-subspaces model to incorporate subspace learning [14], [16], [18]–[20]. Specifically, the spatiotemporal signals measured by the SPICE sequence were modeled by:

$$\rho(\boldsymbol{r},t)=\sum_{n=1}^{N}\sum_{l=1}^{L}u_{n,l}(\boldsymbol{r})v_{n,l}(t) \quad (1)$$

where $\{v_{n,l}(t)\}$ and $\{u_{n,l}(\boldsymbol{r})\}$ denote the lth spectral basis function and its corresponding spatial coefficient of the nth molecule (e.g., water, lipids, and metabolites). With pre-learned spectral basis functions, this model can significantly reduce the degrees-of-freedom needed to represent the spatiotemporal distributions, thus enabling the processing methods to overcome the sparse sampling and noise issues. Specifically, the water and lipid basis functions were estimated from a set of high-resolution non-water-suppressed MRSI data; and the metabolite basis functions were estimated from a set of low-resolution, water-suppressed MRSI data [18], [24], [25]. With the pre-learned water and lipid subspaces and coil sensitivity maps, the sparsely sampled data in peripheral (k, t)-space (for water and lipid signals only) can be recovered. Reconstruction of the desired metabolite signals from the noisy data was accomplished by utilizing the learned metabolite subspaces:

$$\widehat{U}_m=\arg\min_{U_m}\|d-\mathcal{F}(U_mV_m)\|_2^2+\lambda_m\|DU_m\|_2^2 \quad (2)$$

where V_m and U_m represent the spectral basis functions of metabolites and the corresponding spatial coefficients, and λ_m is the regularization parameter. Finally, spectral quantification of the reconstructed metabolite signals was done utilizing an improved LCModel-based method by exploiting the union-of-subspaces model, incorporating both spatial and spectral priors [18].

2) Quantitative T_2 Mapping

In practice, there always exist B_1 inhomogeneity and imperfection in the 180° refocusing pulses used in the TSE sequence. As a result, the T_2-weighted data obtained would not follow a simple exponential model of T_2 relaxation and the T_2 values estimated with only 3 TEs would contain significant errors. To address this problem, we corrected the estimation bias via a model-based approach incorporating a set of pre-acquired calibration data [26]. More specifically, we modelled the deviation between the measured and reference T_2 decays as an echo time shift using the following model:

$$\rho_{\mathrm{meas}}(\boldsymbol{r},T)=\rho_{\mathrm{ref}}(\boldsymbol{r},T)e^{-\frac{\Delta T(r,T)}{T_2(r)}} \quad (3)$$

where $\rho_{\mathrm{meas}}(\boldsymbol{r},T)$ and $\rho_{\mathrm{ref}}(\boldsymbol{r},T)$ are the measured and reference T_2-weighted images, respectively. The reference images are assumed to follow the ideal exponential T_2 evolution; ΔT is the TE shift accounting for the deviation caused by nonideal experimental conditions. To estimate the TE shift, first we generated the calibration T_2 map, $T_{2,\mathrm{cali}}(\boldsymbol{r})$, of the calibration data with 15 TEs (18 to 142 ms, on healthy subjects), $\rho_{\mathrm{cali}}(\boldsymbol{r},T)$, utilizing a dictionary matching method. The dictionary was created by Bloch simulation [8], considering both T_2 evolution and B_1 field inhomogeneity. The generated calibration T_2 maps were then used to synthesize the reference T_2-weighted images of the calibration dataset, $\rho_{\mathrm{rcal}}(\boldsymbol{r},T)$, using the following model:

$$\rho_{\mathrm{rcal}}(\boldsymbol{r},T)=\rho_{\mathrm{cali}}(\boldsymbol{r},T_0)e^{-\frac{T-T_0}{T_{2,\mathrm{cali}}(r)}} \quad (4)$$

The TE-correction maps of the three measured TEs (18, 36, 62 ms), $\Delta T(\boldsymbol{r},T)$, were consequently generated by comparing $\rho_{\mathrm{rcal}}(\boldsymbol{r},T)$ and $\rho_{\mathrm{cali}}(\boldsymbol{r},T)$:

$$\Delta T(\boldsymbol{r},T)=-\ln\left(\frac{\rho_{\mathrm{rcal}}(\boldsymbol{r},T)}{\rho_{\mathrm{cali}}(\boldsymbol{r},T)}\right)\cdot T_{2,\mathrm{cali}}(\boldsymbol{r}) \quad (5)$$

After obtaining the TE-correction maps, we utilized the mean of the TE-correction maps as the TE-shifts for the measured TSE data, since the TE-correction values were spatially smooth and relatively consistent for different data. Finally, the bias-corrected T_2 maps were generated via a typical exponential fitting method using the shifted TE values.

C. Experiments

To demonstrate the feasibility and potential of the proposed methods, in vivo experiments were carried out on healthy subjects and ischemic stroke patients. All MR scans were performed on a 3T Siemens Skyra MRI scanner (Siemens, Erlangen, Germany) with a 20-channel head and neck coil.

To validate the feasibility of the proposed approach on healthy subjects, nineteen adults (age ranged from 25 to 64 years; 13 females) were recruited and underwent MRI scans using the SPICE and TSE sequences. The calibration data for T_2 bias correction were acquired using the same TSE sequence with 15 TEs (TE = [18:9:142] ms). 3D MPRAGE (TR/TE/TI = 2400/2.13/1100 ms, resolution = 1 × 1 × 1 mm^3, FOV = 256 mm, slice number = 192) scan was also acquired for anatomical imaging.

To demonstrate the feasibility and potential of the proposed approach for prediction of stroke symptom onset time in the clinical setting, 56 acute ischemic stroke patients (age ranged from 34 to 88 years; 18 females) were included in this study. Patients were included if they had a clinically confirmed ischemic stroke and presented with known duration of symptomatic ischemia. Exclusion criteria included the presence of contraindication for MRI, evidence of haemorrhagic transformation, or significant non-stroke lesions on structural MRI. All patients underwent MRI and MRSI within 1 week after stroke symptom onset (symptomatic ischemia duration ranged from 2.25 to 135 hours). This study was approved by the Institutional Review Board of the Fifth People's Hospital of Shanghai (Shanghai, People's Republic of China). All participants or their guardians provided written informed consents. The standard scan protocol included 3D MPRAGE (TR/TE/TI = 2400/2.13/1100 ms, resolution = 1 × 1 × 1 mm^3, FOV = 256 mm, slice number = 192), diffusion weighted imaging (DWI) (TR/TE = 4300/[74, 125] ms, resolution = 1.3 × 1.3 × 4 mm^3, FOV = 240 mm, slice number = 25, b = 0 and 1000 s/mm^2), and FLAIR imaging (TR/TE/TI = 9000/89/2500

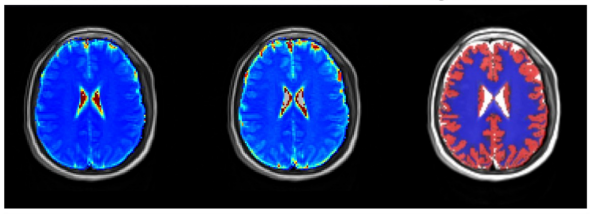

	Before Correction (ms)	After Correction (ms)	T_2 values in Literature (ms)
White Matter	68.3 ± 2.1	81.5 ± 3.0	79.6 ± 0.6
Gray Matter	88.5 ± 2.3	112.6 ± 3.6	110.0 ± 2.0

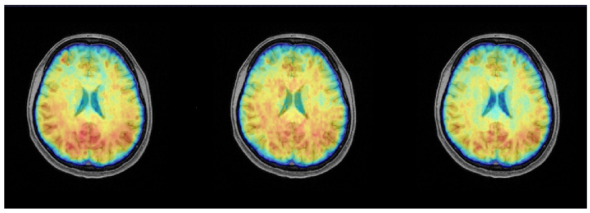

	NAA	Choline	Creatine
GM/WM in Our Data	1.07 ± 0.05	0.99 ± 0.04	1.20 ± 0.06
GM/WM in Literature	0.98 ± 0.08	0.83 ± 0.17	1.20 ± 0.15

Fig. 2. (A) Quantitative T_2 values in white matter (blue) and gray matter (red) acquired from 19 healthy subjects, before and after bias correction using our proposed method. (B) The relative ratios of NAA, choline, and creatine levels in gray matter over white matter acquired from 19 healthy subjects, in comparison with literature values.

ms, resolution = 0.5 × 0.5 × 2 mm^3, FOV = 240 mm, slice number = 82).

D. Data Analysis

For the healthy subjects, we performed region of interest (ROI)-based analysis to compare the mean T_2 values and neurometabolite levels in gray matter and white matter tissues. The ratios between neurometabolite levels in gray matter and white matter were also calculated. Anatomical images were coregistered to the MRSI and T_2 maps using affine linear transformation with 12 degrees of freedom embedded in FMRIB's Linear Image Registration Tool [27], respectively. Gray matter and white matter masks were generated based on the coregistered anatomical images using unified segmentation method embedded in the Statistical Parametric Mapping brain imaging analysis software (SPM12). Independent sample *t*-tests were used for the comparisons.

For stroke patients, the ischemic lesion was manually delineated on the DWI images by an experienced neuroradiologist (T.W. with 10 years of experience). For each patient, T_2 images, as well as the lesion masks, were all coregistered to the MRSI maps using affine linear transformation. Regions for contralateral comparison were created by transforming the lesion masks to standard MNI152 space, flipping along the midline, and transforming back to the native image space. All the registration results were inspected by an experienced neuroradiologist.

The patients were divided into a hyperacute (0 – 24h, $n = 23$) and an acute (24h – 7d, $n = 33$) group [28], [29]. For each patient, the mean T_2 value and neurometabolite levels were calculated within the DWI lesion and contralateral region. For comparisons between lesional and contralateral regions, paired t-tests were performed for the region-wise analyses. To investigate the sensitivity of the lesional multispectral signals to the stroke symptomatic duration, we performed both group-level comparison and correlation analysis. The group-level comparisons were performed between hyperacute and acute groups using independent samples *t*-tests. Pearson correlation analyses were performed to analyze the correlation between the multispectral signals and duration, in which the log-transformed duration was used to reduce the skewness of data. Bonferroni correction was used for multiple comparisons.

To compare the predictive models of symptomatic duration based on our multimodal imaging data (neurometabolites and quantitative T_2), we used Bayesian linear regression employing incrementally increasing numbers of inputs [30]. The widely applicable information criterion (WAIC) was used for model selection [31], [32]. All the statistical analyses were carried out using R software (version 4.0.5) and SPSS 26 (IBM). The Bayesian analysis was implemented with Bayesreg in MATLAB [33].

III. Results

A. 3D MRSI and Quantitative T_2 Mapping in Healthy Subjects

The feasibility of our proposed 3D MRSI and quantitative T_2 mapping was validated in 19 healthy subjects (age: 40.3±12.1 years). As shown in Fig. 2(A), the estimation of T_2 values were significantly improved after bias correction. The mean T_2 values measured in white matter and gray matter after correction were 81.5±0.3 ms and 112.6±3.6 ms, respectively, in line with those reported in the literatures (79.6±0.6 ms for white matter and 110.0 ± 2.0 ms for gray matter) [34].

This article has been accepted for publication in IEEE Transactions on Biomedical Engineering. This is the author's version which has not been fully edited and content may change prior to final publication. Citation information: DOI 10.1109/TBME.2023.3277546

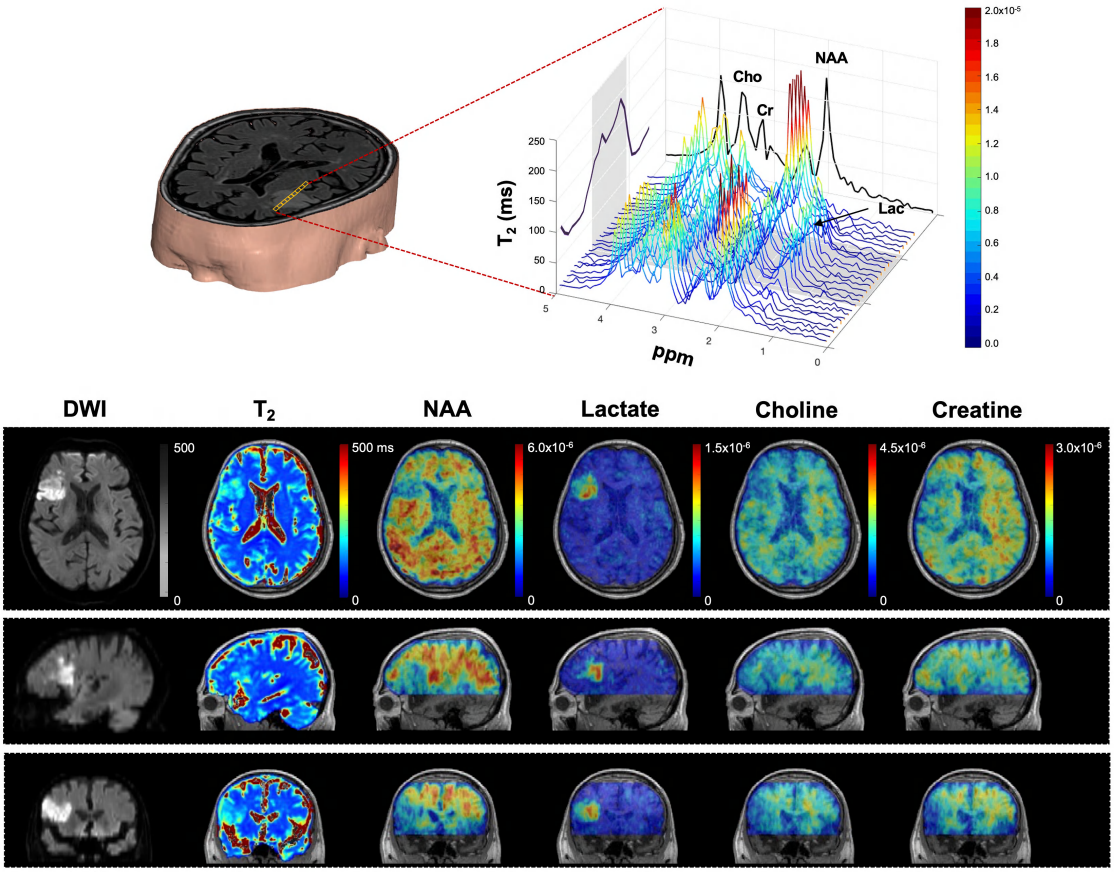

Fig. 3. 3D T_2 maps (spatial resolution of 1.9 × 1.9 × 3.0 mm^3) and 3D metabolite maps (nominal spatial resolution of 2.0 × 3.0 × 3.0 mm^3) of an acute ischemic stroke patient (post-stroke onset time: 54.27 h). The T_2 maps were obtained in a 69-second scan and the metabolite maps in an 8-minute scan using the proposed method. The representative spectra were obtained from the marked region (consecutively across the peripheral to central lesion regions). The color bar for spectra shows the amplitude of the metabolite signal. Representative multimodal images are illustrated in axial, sagittal and coronal views (from top to bottom). The color bar for the T_2 maps shows the T_2 value in ms. The color bar for the metabolite maps shows NAA, lactate, choline, or creatine levels in institutional units.

Representative neurometabolites maps including NAA, choline and creatine of one healthy subject were displayed in Fig. 2(B). The gray matter and white matter ratios of NAA, choline and creatine were 1.07 ± 0.05, 0.99 ± 0.04, and 1.20 ± 0.06, respectively, which are consistent with those in the literatures (0.98 ± 0.08 for NAA, 0.83 ± 0.17 for choline, and 1.20 ± 0.15 for creatine) [10].

B. 3D MRSI and Quantitative T_2 Mapping in Acute Stroke Patients

High-resolution 3D neurometabolite and T_2 maps from a representative acute stroke patient (duration of symptomatic ischemia: 54.27 h) are shown in Fig. 3. The 3D spectra clearly showed reduced NAA and increased lactate levels along with an increase of T_2 value in the lesion. Representative neurometabolite and quantitative T_2 maps from six different ischemic stroke patients with onset time from 2.25 to 107 hours are shown in Fig. 4 in the order of increasing time after onset, along with the corresponding DWI and FLAIR images. A decrease in NAA, and an increase in both lactate and T_2 values can be observed within the lesion compared to the contralateral side. The increase in T_2 and decrease in NAA along with patients' symptom onset time are also apparent in these cross-sectional data.

The comparisons of the changes in neurometabolite levels and T_2 values between the hyperacute and acute groups are shown in Fig. 5. In both groups, the lesional T_2 values were higher than those in the contralateral region ($p < 0.001$). In the hyperacute group, decreased NAA and increased lactate levels were shown in the lesion (all $p < 0.001$). In the acute group, decreased lesional NAA, choline, and creatine as well as increased lesional lactate were shown (all $p < 0.001$). The lesional T_2 value of the hyperacute group was lower compared to acute group ($p < 0.001$). The lesional creatine level of the hyperacute group was higher compared to acute group ($p = 0.001$). The difference in lesional NAA, choline, and lactate levels between hyperacute and acute groups did not reach significant level (NAA: $p = 0.086$; choline: $p = 0.103$; lactate: $p = 0.149$).

C. Correlation between Neurometabolites and Quantitative T_2 Values with Symptom Onset Time

The correlations of several biomarkers with symptom onset time are shown in Fig. 6. As can be seen, increased T_2 value and decreased NAA, choline and creatine levels were all

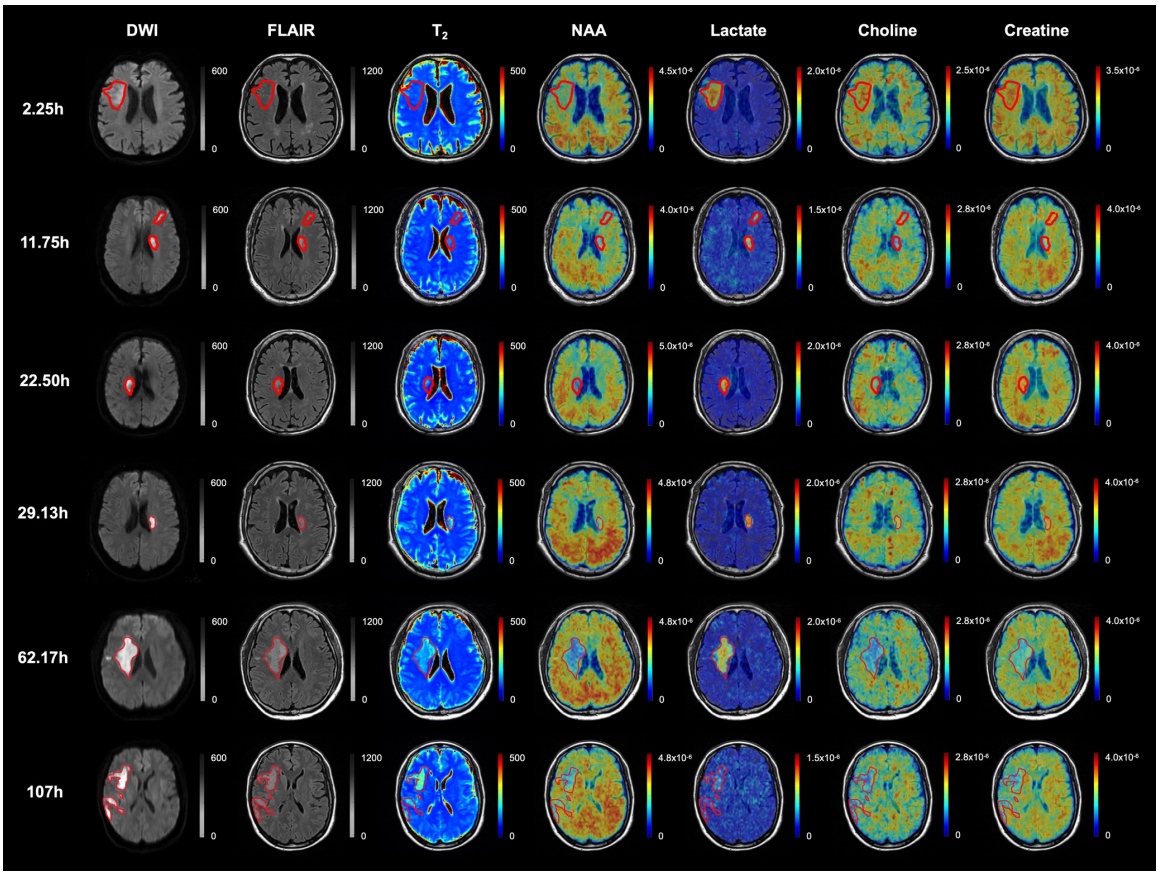

Fig. 4. Multimodal images from six representative stroke patients with different symptom durations from hyperacute to acute stages. The color bar for T_2 mapping shows the T_2 value in ms. The color bar for metabolite maps shows NAA, lactate, choline, or creatine levels in institutional units. Lesions were contoured by red lines.

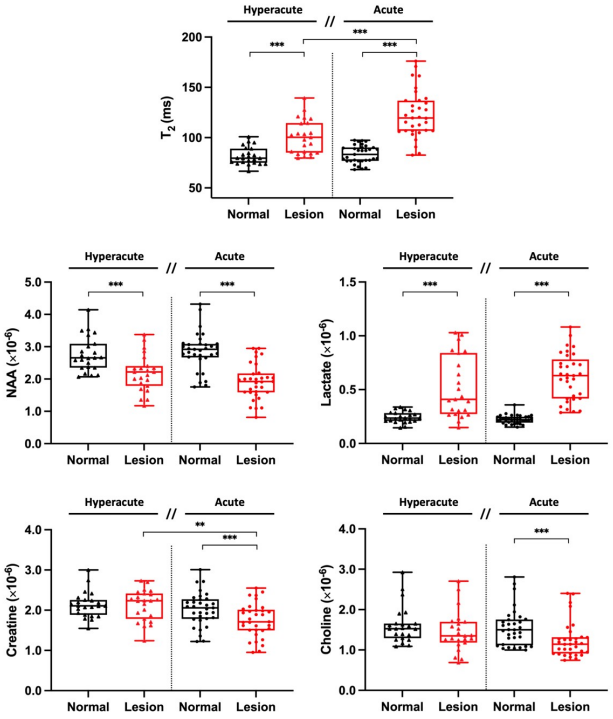

Fig. 5. Comparisons of mean T_2 values and neurometabolite levels between DWI lesion and contralateral regions in hyperacute and acute stroke patients. Each data point represents one patient data. ** = $p < 0.01$, *** = $p < 0.001$ with Bonferroni-corrected *t*-test.!

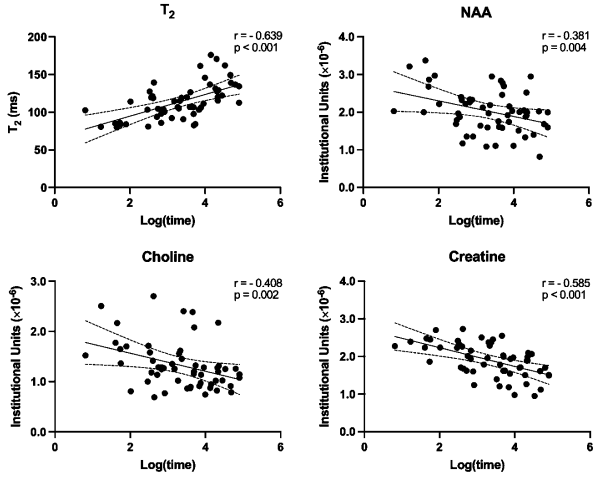

Fig. 6. Scatter plots of the correlations between lesional T_2 values and neurometabolite levels with symptomatic ischemia duration for all stroke patients. All results are adjusted with age. Time (h) is log-transformed to reduce the skewness of data distribution.!

significantly correlated with the duration of symptomatic ischemia (T_2: $r = 0.639$, $p < 0.001$; NAA: $r = -0.381$, $p = 0.004$; choline: $r = -0.408$, $p = 0.002$; creatine: $r = -0.585$, $p < 0.001$). Taken together, the lesional T_2, NAA, choline, and creatine levels all showed their sensitivity to the duration of ischemic damage.

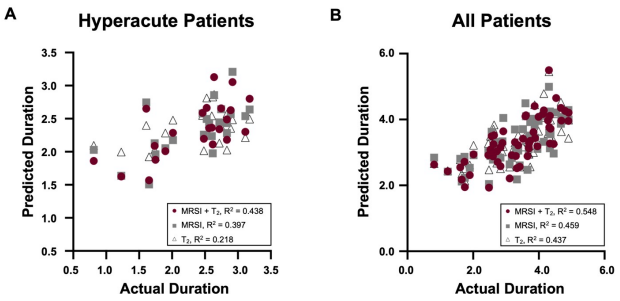

Fig. 7. Prediction of symptomatic ischemia duration in (A) hyperacute and (B) all stroke patients, respectively. Time (h) is log-transformed to reduce the skewness of data distribution.!

D. Prediction of Symptom Onset Time using Multispectral Signals

We investigated whether the combination of neurometabolites and T_2 values could improve the prediction of symptomatic duration for hyperacute stroke (n = 23) as well as for all patients (n = 56). The results are shown in Fig. 7. In the hyperacute group, the best prediction performance (R^2 = 0.438, WAIC = 25.630) was achieved when combining all imaging biomarkers, in comparison with MRSI (R^2 = 0.397, WAIC = 25.243) or T_2 alone (R^2 = 0.218, WAIC = 23.848). Across all patients, we also achieved the best prediction performance (R^2 = 0.548, WAIC = 65.990) when combining all imaging biomarkers, in comparison with MRSI (R^2 = 0.459, WAIC = 69.791) or T_2 alone (R^2 = 0.437, WAIC = 67.755). Additionally, the winning models also exhibited the lowest WAIC, indicating the best balance of flexibility and fit.

IV. Discussion

The multifactorial nature of stroke pathology motivates a multispectral imaging approach, to characterize the lesion across multiple dimensions that directly index the complex underlying neurochemical changes, with high spatial resolution, and within short acquisition times. To the best of our knowledge, the current study is the first to demonstrate the feasibility of combined high-resolution 3D MRSI and quantitative T_2 mapping of stroke patients in the clinical setting. Our proposed clinically applicable approach enables investigation of the pathophysiological interactions between the development of vasogenic oedema, tissue acidosis, and neuronal/glial cells damage within lesion and yields improved diagnostic and prognostic accuracy.

Previous MRS/MRSI techniques in stroke studies were constrained by limited imaging volume, poor resolution, and long acquisition time, which largely impeded their clinical applications [8]. Specifically, most of the current practically used MRS/MRSI methods take more than 15-minute scan times and the voxel sizes are usually around 1 cm^3, constraining their applications in clinical stroke studies. Building on the previous work [35], in this study, we leveraged high-resolution 3D MRSI along with quantitative T_2 mapping on a cohort of ischemic stroke patients across hyperacute and acute stages to explore the feasibility of such a multimodal imaging approach in stroke clinical settings. Multiple neurometabolite maps including NAA, lactate, choline, and creatine were acquired at a nominal spatial resolution of 2 × 3 × 3 mm^3 using the SPICE sequence, which could minimize the partial volume effects, provide high SNR, and allow good delineation of neurometabolite maps within the lesion area. It is worth to mention that our MRSI data are T_1-weighted due to the short TR used for fast scanning. Even with the T_1 effect, we still observed strong contrast of both NAA and lactate within the lesion in our current study. Further research is necessary to remove the T_1-weighted effect if desired for prediction of stroke onset time.

The TSE sequence is widely used in stroke applications due to its time efficiency compared to the conventional SE sequence [36]. Previous works usually used TSE with more than 10 TEs to achieve accurate quantitative T_2 maps, which required a total acquisition time more than 10 minutes [37]. To better satisfy the clinical need for stroke studies, our TSE sequence used parallel imaging and reduced the number of TEs (to only 3) to accelerate data acquisition, resulting in a scan time of around one minute. The associated T_2 estimation bias issue was solved using a model-based method, making accurate T_2 mapping using only 3 TEs possible. This model-based method modelled the imperfections/bias as TE shifts and used a set of calibration data to pre-determine the shift values for correction. This set of calibration data only needs to be collected once for the TSE sequence with a specific parameter setup on a specific scanner, thus no additional calibration scans are needed for clinical applications.

Using the proposed multispectral imaging approach, we found consistently increased T_2 values in the lesion of hyperacute and acute stroke patients, which has been attributed to the development of vasogenic edema typically found up to 7d post stroke onset [5], [38]. Reduced NAA and choline, along with increased lactate levels, were also shown in the lesion of both groups. Decreased NAA has been associated with neuronal/axonal loss or mitochondrial dysfunction; decreased choline might be related to disrupted metabolic pathway for the membrane maintenance due to the energy breakdown post occlusion [39]. The increased lactate in hyperacute stroke reflects the anaerobic glycolysis in potentially viable neuronal or glia cells, while infiltrating macrophages might lead to persistent lactate increase at a later stage of stroke [40]. As a marker of disrupted energy metabolism, the reduction in creatine was observed in the acute stroke group. Since creatine is present in both neuronal and glial cells, and the glial cells are known to be more resistant to ischemia, this might explain the delayed reduction in creatine level [41].

The lesion T_2 increases were associated with symptomatic duration in both hyperacute and acute stroke patients, indicating its sensitivity to lesion age [5]. The NAA reduction was correlated to the duration of symptomatic ischemia in hyperacute stroke patients, indicating the time-dependent neuronal damage of cerebral infarction. In the acute stroke group, the reduction in creatine was significantly correlated with the symptom onset time, indicating a time-dependent loss of glial cells within this window [42]. When considering all the patients, the changes in lesional NAA, choline, creatine, and T_2 were all correlated with lesion age, showing their sensitivity to

the duration of ischemic damage. When combining 3D metabolic and T_2 mapping, we obtained the best predictive power of symptomatic ischemia duration, indicating an improved assessment of pathological changes in ischemic tissues as well as a potential guidance of time-sensitive therapies post stroke.

Several limitations should be noted. Although the current study demonstrated the feasibility of combined metabolic and T_2 mapping, both data were acquired using separate sequences, which may cause registration errors. Development of technology for simultaneous acquisitions would avoid any potential image registration error. Second, the current T_2 correction method only corrects the spatially low-order bias caused by the system imperfections. Including deep learning may provide possibility for higher-order correction of the bias. Third, the relatively small number of patients studied will need to be replicated at larger scale to assure generalisability. Forth, denser sampling of the early hyperacute window would be valuable, given its interventional relevance. Nonetheless, it is noteworthy that in addition to mechanical thrombectomy and tissue plasminogen activators (tPA), other interventions such as transcranial direct current stimulation have been shown to improve functional outcome of the patients following acute stroke within 7d post stroke [43].

V. Conclusion

Using combined fast high-resolution 3D MRSI and T_2 mapping, we captured the concomitant changes in quantitative T_2 value and NAA, creatine, and choline levels in hyperacute and acute cerebral infarctions of ischemic stroke patients. The multimodal signals improved the predictions of symptomatic ischemia duration in all stroke patients. Our results demonstrate the feasibility of combined high-resolution 3D metabolic imaging with quantitative T_2 mapping in clinical settings and show that multimodal image data improves the assessment of the duration of cerebral infarction.

References

[1] A. Wouters *et al.*, "Prediction of stroke onset is improved by relative fluid-attenuated inversion recovery and perfusion imaging compared to the visual diffusion-weighted imaging/fluid-attenuated inversion recovery mismatch," *Stroke*, vol. 47, no. 10, pp. 2559–2564, Oct. 2016.

[2] G. Thomalla *et al.*, "MRI-guided thrombolysis for stroke with unknown time of onset," *N. Engl. J. Med.*, vol. 379, no. 7, pp. 611–622, Aug. 2018.

[3] P. B. Barker *et al.*, "Acute stroke: Evaluation with serial proton MR spectroscopic imaging," *Radiology*, vol. 192, no. 3, pp. 723–732, Sep. 1994.

[4] S. M. Maniega *et al.*, "Changes in NAA and lactate following ischemic stroke: A serial MR spectroscopic imaging study," *Neurology*, vol. 71, no. 24, pp. 1993–1999, Dec. 2008.

[5] S. Siemonsen *et al.*, "Quantitative T_2 values predict time from symptom onset in acute stroke patients," *Stroke*, vol. 40, no. 5, pp. 1612–1616, May 2009.

[6] F. Nicoli, Y. Lefur, B. Denis, J. P. Ranjeva, S. Confort-Gouny, and P. J. Cozzone, "Metabolic counterpart of decreased apparent diffusion coefficient during hyperacute ischemic stroke," *Stroke*, vol. 34, no. 7, pp. e82–e87, Jul. 2003.

[7] V. Cvoro *et al.*, "Associations between diffusion and perfusion parameters, N-acetyl aspartate, and lactate in acute ischemic stroke," *Stroke*, vol. 40, no. 3, pp. 767–772, Mar. 2009.

[8] N. Ben-Eliezer, D. K. Sodickson, and K. T. Block, "Rapid and accurate T_2 mapping from multi-spin-echo data using Bloch-simulation-based reconstruction," *Magn. Reson. Med.*, vol. 73, no. 2, pp. 809–817, Feb. 2015.

[9] J. M. Wild, J. M. Wardlaw, I. Marshall, and C. P. Warlow, "N-acetylaspartate distribution in proton spectroscopic images of ischemic stroke," *Stroke*, vol. 31, no. 12, pp. 3008–3014, Dec. 2000.

[10] A. A. Maudsley *et al.*, "Mapping of brain metabolite distributions by volumetric proton MR spectroscopic imaging (MRSI)," *Magn. Reson. Med.*, vol. 61, no. 3, pp. 548–559, Mar. 2009.

[11] S. Majumdar, A. Gmitro, S. C. Orphanoudakis, D. Reddy, and J. C. Gore, "An estimation and correction scheme for system imperfections in multiple-echo magnetic resonance imaging," *Magn. Reson. Med.*, vol. 4, no. 3, pp. 203–220, Mar. 1987.

[12] S. Majumdar, S. C. Orphanoudakis, A. Gmitro, M. O'Donnell, and J. C. Gore, "Errors in the measurements of T_2 using multiple-echo MRI techniques. I. Effects of radiofrequency pulse imperfections," *Magn. Reson. Med.*, vol. 3, no. 3, pp. 397–417, Jun. 1986.

[13] J. Hennig, "Multiecho imaging sequences with low refocusing flip angles," *J. Magn. Reson.*, vol. 78, no. 3, pp. 397–407, Jul. 1988.

[14] Z. P. Liang, "Spatiotemporal imaging with partially separable functions," in *Proceedings of the 4th IEEE International Symposium on Biomedical Imaging: From Nano to Macro*, 2007, pp. 988–991.

[15] F. Lam and Z. P. Liang, "A subspace approach to high-resolution spectroscopic imaging," *Magn. Reson. Med.*, vol. 71, no. 4, pp. 1349–1357, Feb. 2014.

[16] F. Lam, C. Ma, B. Clifford, C. L. Johnson, and Z. P. Liang, "High-resolution ^{1}H-MRSI of the brain using SPICE: Data acquisition and image reconstruction," *Magn. Reson. Med.*, vol. 76, no. 4, pp. 1059–1070, Oct. 2016.

[17] C. Ma, F. Lam, C. L. Johnson, and Z. P. Liang, "Removal of nuisance signals from limited and sparse ^{1}H-MRSI data using a union-of-subspaces model," *Magn. Reson. Med.*, vol. 75, no. 2, pp. 488–497, Feb. 2016.

[18] Y. Li, F. Lam, B. Clifford, and Z. Liang, "A subspace approach to spectral quantification for MR spectroscopic imaging," *IEEE Trans. Biomed. Eng.*, vol. 64, no. 10, pp. 2486–2489, Oct. 2017.

[19] X. Peng, F. Lam, Y. Li, B. Clifford, and Z. P. Liang, "Simultaneous QSM and metabolic imaging of the brain using SPICE," *Magn. Reson. Med.*, vol. 79, no. 1, pp. 13–21, Jan. 2018.

[20] R. Guo, Y. Zhao, Y. Li, Y. Li, and Z. P. Liang, "Simultaneous metabolic and functional imaging of the brain using SPICE," *Magn. Reson. Med.*, vol. 82, no. 6, pp. 1993–2002, Dec. 2019.

[21] R. Guo *et al.*, "Simultaneous QSM and metabolic imaging of the brain using SPICE: Further improvements in data acquisition and processing," *Magn. Reson. Med.*, vol. 85, no. 2, pp. 970–977, Feb. 2021.

[22] F. A. Breuer *et al.*, "Controlled aliasing in volumetric parallel imaging (2D CAIPIRINHA)," *Magn. Reson. Med.*, vol. 55, no. 3, pp. 549–556, Mar. 2006.

[23] A. Seiler *et al.*, "Extent of microstructural tissue damage correlates with hemodynamic failure in high-grade carotid occlusive disease: An MRI study using quantitative T_2 and DSC perfusion," *AJNR. Am. J. Neuroradiol.*, vol. 39, no. 7, pp. 1273–1279, Jul. 2018.

[24] F. Lam, Y. Li, R. Guo, B. Clifford, and Z. P. Liang, "Ultrafast magnetic resonance spectroscopic imaging using SPICE with learned subspaces," *Magn. Reson. Med.*, vol. 83, no. 2, pp. 377–390, Feb. 2020.

[25] R. Guo *et al.*, "High-resolution label-free molecular imaging of brain tumor," *Proc. Annu. Int. Conf. IEEE Eng. Med. Biol. Soc. EMBS*, pp. 3049–3052, 2021.

[26] T. Zhang, R. Guo, Y. Li, Y. Zhao, Y. Li, and Z.-P. Liang, "T_2' mapping of the brain from water-unsuppressed ^{1}H-MRSI and turbo spin-echo data," *Magn. Reson. Med.*, Jul. 2022.

[27] M. Jenkinson, C. F. Beckmann, T. E. J. Behrens, M. W. Woolrich, and S. M. Smith, "FSL," *Neuroimage*, vol. 62, no. 2, pp. 782–790, Aug. 2012.

[28] L. M. Allen, A. N. Hasso, J. Handwerker, and H. Farid, "Sequence-specific MR imaging findings that are useful in dating ischemic stroke," *Radiographics*, vol. 32, no. 5, pp. 1285–1297, Sep. 2012.

[29] J. Bernhardt *et al.*, "Agreed definitions and a shared vision for new standards in stroke recovery research: The Stroke Recovery and Rehabilitation Roundtable taskforce," *Int. J. Stroke*, vol. 12, no. 5, pp. 444–450, Jul. 2017.

[30] V. Rajajee *et al.*, "Early MRI and outcomes of untreated patients with mild or improving ischemic stroke," *Neurology*, vol. 67, no. 6, pp. 980–984, Sep. 2006.

[31] S. Watanabe, "A widely applicable Bayesian information criterion," *arXiv Prepr.*, 2012.

[32] A. K. Bonkhoff *et al.*, "Bringing proportional recovery into proportion: Bayesian modelling of post-stroke motor impairment," *Brain*, vol. 143, no. 7, pp. 2189–2206, Jul. 2020.

[33] E. Makalic and D. F. Schmidt, "High-dimensional Bayesian regularised regression with the BayesReg package," *arXiv Prepr.*, Nov. 2016.

[34] J. P. Wansapura, S. K. Holland, R. S. Dunn, and W. S. Ball, "NMR relaxation times in the human brain at 3.0 Tesla," *J. Magn. Reson. Imaging*, vol. 9, no. 4, pp. 531–538, Apr. 1999.

[35] Y. Li *et al.*, "Fast high-resolution metabolic imaging of acute stroke with 3D magnetic resonance spectroscopy," *Brain*, vol. 143, no. 11, pp. 3225–3233, Nov. 2021.

[36] U. Nöth, M. Shrestha, J. R. Schüre, and R. Deichmann, "Quantitative in vivo T_2 mapping using fast spin echo techniques – A linear correction procedure," *Neuroimage*, vol. 157, pp. 476–485, Aug. 2017.

[37] R. G. Sah *et al.*, "Temporal evolution and spatial distribution of quantitative T_2 MRI following acute ischemia reperfusion injury," *Int. J. Stroke*, vol. 15, no. 5, pp. 495–506, Jul. 2020.

[38] S. Siemonsen *et al.*, "Elevated T_2-values in MRI of stroke patients shortly after symptom onset do not predict irreversible tissue infarction," *Brain*, vol. 135, no. 6, pp. 1981–1989, Jun. 2012.

[39] B. L. Miller, "A review of chemical issues in ^{1}H NMR spectroscopy: N-acetyl-l-aspartate, creatine and choline," *NMR Biomed.*, vol. 4, no. 2, pp. 47–52, Apr. 1991.

[40] G. D. Graham *et al.*, "Proton magnetic resonance spectroscopy of cerebral lactate and other metabolites in stroke patients," *Stroke*, vol. 23, no. 3, pp. 333–340, Mar. 1992.

[41] J. H. Duijn, G. B. Matson, A. A. Maudsley, J. W. Hugg, and M. W. Weiner, "Human brain infarction: Proton MR spectroscopy," *Radiology*, vol. 183, no. 3, pp. 711–718, Jun. 1992.

[42] S. M. Maniega, V. Cvoro, P. A. Armitage, I. Marshall, M. E. Bastin, and J. M. Wardlaw, "Choline and creatine are not reliable denominators for calculating metabolite ratios in acute ischemic stroke," *Stroke*, vol. 39, no. 9, pp. 2467–2469, Sep. 2008.

[43] S. Kumar *et al.*, "Noninvasive brain stimulation may improve stroke-related dysphagia: A pilot study," *Stroke*, vol. 42, no. 4, pp. 1035–1040, Apr. 2011.